nature chemical biology

BRIEF COMMUNICATION

PUBLISHED ONLINE: 6 FEBRUARY 2017 | DOI: 10.1038/NCHEMBIO.2285

Structure and specificity of a permissive bacterial C-prenyltransferase

Sherif I Elshahawi[1,2], Hongnan Cao[3], Khaled A Shaaban[1,2], Larissa V Ponomareva[1,2], Thangaiah Subramanian[4], Mark L Farman[5], H Peter Spielmann[4,6], George N Phillips Jr[3]*, Jon S Thorson[1,2]* & Shanteri Singh[2,7]*

This study highlights the biochemical and structural characterization of the L-tryptophan C6 C-prenyltransferase (C-PT) PriB from *Streptomyces* sp. RM-5-8. PriB was found to be uniquely permissive to a diverse array of prenyl donors and acceptors including daptomycin. Two additional PTs also produced novel prenylated daptomycins with improved antibacterial activities over the parent drug.

Biocatalysts involved in late-stage natural product (NP) tailoring modifications (acylation, alkylation, glycosylation and oxidation) are a centerpiece of a number of successful biocatalytic strategies for non-native modification of complex NP core scaffolds[1–3]. Within this context, microbes from unexplored environments are a rich source for new chemical and biocatalytic diversity[4–7]. Herein we describe the discovery and characterization of PriB, a permissive L-tryptophan (L-Trp) C6 C-prenyltransferase (C-PT) from the Appalachian Kentucky coal-mine-fire-associated *Streptomyces* sp. RM-5-8 isolate[8]. Biochemical and structural studies highlight PriB as a highly proficient and substrate-permissive PT that adopts a substrate-binding orientation distinct from those of most other indole PTs; the antibiotic daptomycin (Cubicin; DAP) was noted among the range of unique PriB acceptors. The indole C4 C-PT FgaPT2 and reverse C3 C-PT CdpNPT were also capable of prenylation and, in conjunction with PriB, provided three distinct novel C- and N-prenylated Trp_1 DAPs. Cumulatively, this study highlights the discovery and characterization of a uniquely permissive C-PT and, for the first time, extends the demonstrated successful application of L-Trp and indole PTs to include C- and N-alkylation of complex cyclic peptides.

Streptomyces sp. RM-5-8 was recently reported to produce two distinct metabolite classes that structurally share a rare unsaturated hexuronic acid (**Fig. 1a**, **2**–**4**)[8]. Whole-genome sequencing of *Streptomyces* sp. RM-5-8 led to a draft genome consisting of 259 contigs with a mean size of 36,940 base pairs (bp) and a GC percentage of 72.1% (**Supplementary Results**, **Supplementary Fig. 1**). Bioinformatic analysis revealed a single putative PT-encoding gene, designated *priB*, clustered with additional genes spanning a region of 25.3 kb (GenBank accession number KT895008; **Supplementary Figs. 1** and **2**; **Supplementary Table 1**) that encode putative functions consistent with the proposed biosynthesis of **2**, including a tryptophanase (*priA*), two cytochrome P450s (*priC/D*) and two transglycosylases (*priE/F*). The *priB* gene was predicted to encode a 385-amino-acid protein (PriB) that belongs to the αββα aromatic PT superfamily (**Supplementary Figs. 3** and **4**; **Supplementary Table 1**) and has close homology to dimethylallyltryptophan synthases (DMATSs)[9,10]. We proposed a biosynthetic pathway for **2** in which PriB catalyzes C6 C-prenylation of L-Trp as an early initiating step (**Fig. 1a**; **Supplementary Fig. 5**). To test this hypothesis, *N*-His_6–PriB (herein referred to as PriB) was heterologously produced in *Escherichia coli* and purified to homogeneity. Analytical-scale reactions with L-Trp and dimethylallyl pyrophosphate (DMAPP) led to PriB-dependent quantitative conversion to a new prenylated product, as detected by HPLC-MS, consistent with the putative function of L-Trp C-PT or DMATS (**Supplementary Fig. 6**). Reaction optimization revealed that PriB displayed relatively broad metal, temperature and pH tolerance (**Supplementary Figs. 7** and **8**). Preparative-scale reactions and preparative HPLC led to a single prenylated product (80% isolated yield). HR–ESI–MS and NMR (**Supplementary Fig. 9**; **Supplementary Table 2**) confirmed the product as **1** (**Fig. 1a**), thereby validating the C6 C-PT function of PriB. Reminiscent of results obtained with the PTs IptA and SAML0654 (refs. 11,12), replacing L-Trp with 6-methyl-Trp (**Fig. 1b**, **5**; a substrate in which the C6 alkylation site is blocked) in the PriB-catalyzed reaction led to efficient (62% conversion) PriB-catalyzed C7 prenylation (**Fig. 1b**; **Supplementary Figs. 9**–**11**; **Supplementary Table 3**), highlighting the potential for substrate-based modulation of PriB regiospecificity. PriB steady-state kinetic parameters (L-Trp: k_{cat} = 77.7 ± 1.3 min^{-1}, $K_m = 1.1 \pm 0.05\,\mu M$; DMAPP: $k_{cat} = 105.6 \pm 7.6\,min^{-1}$, $K_m = 2.0 \pm 0.35\,\mu M$) implicated PriB as being notably proficient among kinetically characterized DMATSs (**Supplementary Table 4**).

To further probe PriB substrate specificity, a range of potential acceptors (**Fig. 1b**; **Supplementary Figs. 10** and **11**; **Supplementary Table 5**) and donors (**Fig. 1c**; **Supplementary Figs. 12**–**16**; **Supplementary Table 6**) was evaluated under saturating native donor DMAPP or acceptor L-Trp, respectively. PriB catalyzed prenylation of Trp analogs, simple indoles and dihydroxynaphthalenes previously identified as DMATS substrates[9], and also revealed a number of additional acceptors beyond the established scope of DMATSs, including anthranilic acid (**28**), uniquely functionalized naphthalenes (**24**), anthraquinones (**23**), phenazines (**22**) and the drug pindolol (**20**; Visken). PriB is also the first DMATS capable of quantitative conversion of both L- and D-Trp. Reminiscent of the phenolic O-PT SirD capable of C-, N- and S-prenylation[13], PriB catalyzed mono- and diprenylation of 5-hydroxy-L-Trp (**Fig. 1b**, **7**), implicating its potential for O-alkylation. Unlike most other PTs[9], PriB displayed flexibility toward longer prenyl donors, including geranyl diphosphate (C10; **Fig. 1c**, **29**), farnesyl diphosphate (C15; **Fig. 1c**, **30**) and geranylgeranyl diphosphate (C20; **Fig. 1c**, **31**).

[1]Department of Pharmaceutical Sciences, College of Pharmacy, University of Kentucky, Lexington, Kentucky, USA. [2]Center for Pharmaceutical Research and Innovation (CPRI), University of Kentucky, Lexington, Kentucky, USA. [3]Department of Biosciences, Rice University, Houston, Texas, USA. [4]Department of Molecular and Cellular Biochemistry, University of Kentucky, Lexington, Kentucky, USA. [5]Department of Plant Pathology, University of Kentucky, Lexington, Kentucky, USA. [6]Department of Chemistry, Markey Cancer Center, Kentucky Center for Structural Biology, University of Kentucky, Lexington, Kentucky, USA. [7]Present address: Department of Chemistry and Biochemistry, University of Oklahoma, Norman, Oklahoma, USA. *e-mail: shanteri.singh@ou.edu, jsthorson@uky.edu or georgep@rice.edu

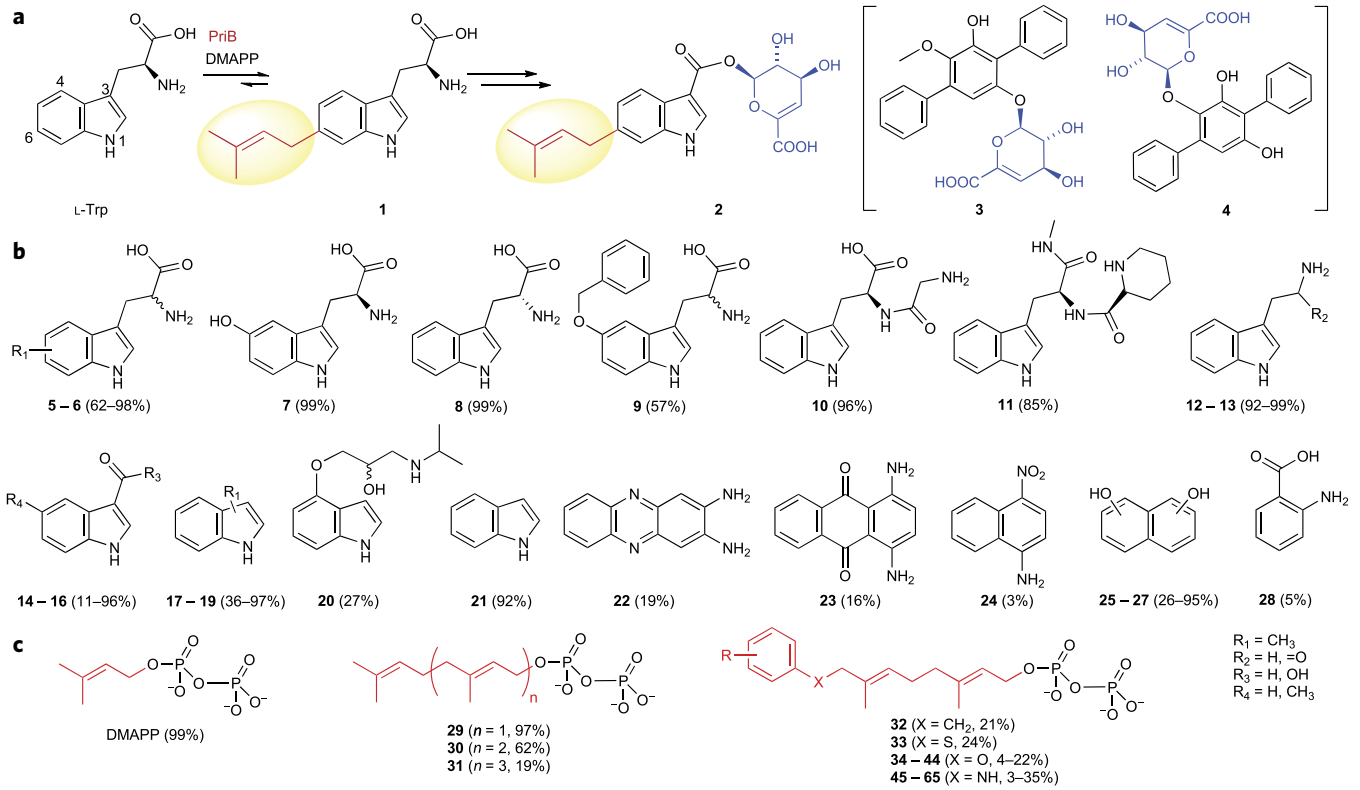

Figure 1 | PriB discovery and permissiveness of PriB and other indole PTs. (**a**) Genome mining revealed the putative locus for the biosynthesis of **2**, including PriB. (**b**,**c**) Substrate permissiveness of PriB. Percent conversion (in parentheses) of enzyme reactions containing constant native donor (dimethylallyl pyrophosphate, DMAPP) and variable prenyl acceptors (**5**–**28**) (**b**) or constant native acceptor (L-Trp) and variable donors (**29**–**65**) (**c**) (*n* = 2; see also **Supplementary Figs. 10**–**16**; **Supplementary Tables 5**–**6**).

To date, similar donor permissiveness has only been reported for the indolactam V–specific PTs TleC and MpnD[14]. PriB also catalyzed turnover with 34 farnesyl diphosphate mimetics[15] (**Supplementary Figs. 13** and **14**; **Supplementary Table 6**), including phenoxy-, anilino-, phenylsulfanyl- and benzyl-substituted analogs (**Fig. 1c**, **32**–**65**; **Supplementary Figs. 15** and **16**), in the first example of PT-catalyzed utilization of diverse non-native farnesyl diphosphate surrogates. While both acceptor- and, to a lesser extent, donor-permissive DMATSs have been reported[9,13,14], PriB is among the most proficient and permissive to date.

Inspired by PriB's permissiveness, we assessed its potential to utilize the more complex structure of DAP[16], which contains both L-Trp- and anthranilate (**28**)-related PriB recognition elements. Analytical-scale reactions using DAP and DMAPP revealed the formation of a new product (~11% turnover) consistent with DAP prenylation, as observed by LC–MS (**Fig. 2a**; **Supplementary Fig. 17**). Similar DAP-based prenylation assays with six other PTs (**Supplementary Figs. 18** and **19**; **Supplementary Table 7**) revealed that both FgaPT2 (an indole C4 C-PT[17]) and CdpNPT (an indole reverse C3 C-PT, originally annotated as an N-PT[18]) also successfully catalyzed DAP prenylation (65% and 75% (**Supplementary Figs. 20** and **21**) conversion, respectively). Preparative reactions and preparative HPLC led to single prenylated products from the PriB- and FgaPT2-catalyzed reactions (6% and 15% isolated yield, respectively). HR–ESI–MS and NMR confirmed the PriB-catalyzed product as the 6-*C*-prenyl-Trp$_1$ DAP (**66**) and the FgaPT2-catalyzed product as the *N*-prenyl-Trp$_1$ DAP (**67**; **Fig. 2a**; **Supplementary Figs. 22**–**24**; **Supplementary Table 8**; **Supplementary Note**). Interestingly, similar CdpNPT-catalyzed preparative-scale reactions and characterization revealed an inseparable 1:1 mixture (**Fig. 2a**; 54 mg, 70% isolated yield) of **67** and the unusual C3 reverse prenyl product **68** (a putative pathway in **Supplementary Fig. 25**). Given the distinction between previously reported FgaPT2 and CdpNPT PT regiospecificity and that determined in the context of DAP, the products of preparative-scale FgaPT2 and CdpNPT reactions with L-Trp were re-evaluated. Consistent with the literature, this analysis confirmed that FgaPT2 is a catalyst for L-Trp C4 prenylation (**Supplementary Fig. 26**; **Supplementary Table 9**) and that turnover of L-Trp by CdpNPT is poor (yielding insufficient product for characterization). Subsequent antimicrobial susceptibility studies comparing **66**–**68** to DAP revealed *C*6- or *N*-Trp$_1$-prenylation (**66** or **67**, respectively) to invoke a 6- to 10-fold improvement in antibacterial activity (with no apparent change in general cytotoxicity; **Supplementary Table 10**), implicating increased lipophilicity as a potential contributor, consistent with previously reported DAP structure–activity relationship (SAR) studies[19]. In addition to offering new improved DAP analogs, this discovery sets the stage for the exploration of additional non-native macromolecular peptide- and/or protein-based targets.

To investigate the structural basis for PriB substrate specificity and catalysis, the X-ray crystal structures of apo-PriB (PDB ID 5JXM), the PriB–pyrophosphate binary complex (PDB ID 5K9M) and a PriB–L-Trp–dimethylallyl *S*-thiolodiphosphate ternary complex (PDB ID 5INJ) were determined at 1.15, 1.50 and 1.40 Å resolution, respectively (**Supplementary Table 11**). In a structure reminiscent of the PT-barrel fold of aromatic and indole PTs[20,21] (**Supplementary Fig. 27**), PriB is comprised of a central β-barrel, formed by a cylindrical β-sheet arranged around a solvent-filled core, surrounded by a ring of solvent-exposed α-helices. A comparison of apo-PriB to ligand-bound structures revealed substantial side chain rearrangement (notably, 123° and 34° rotation of Arg108 and Tyr181, respectively) within the active site and the loop regions around the active site upon substrate binding that were mediated via both key hydrophobic and hydrogen

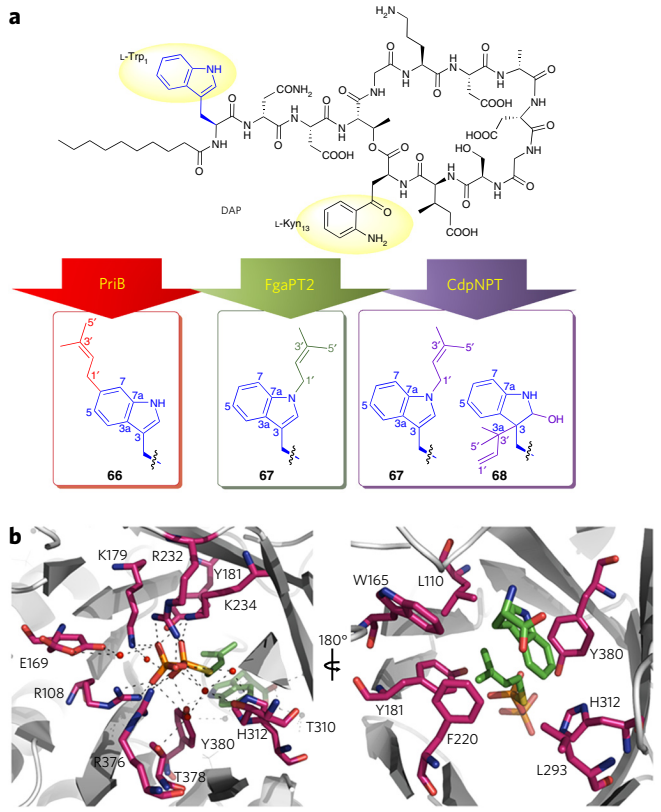

Figure 2 | Prenylated daptomycins (DAPs) and the crystal structure of PriB. (**a**) Products of PriB-, FgaPT2- and CdpNPT-catalyzed prenylation of DAP. (**b**) PriB active site residues and corresponding ligand hydrogen bond interactions (left, front and right, back perspective). The ligands are illustrated as ball-and-stick models, with the following color code: carbon, green; oxygen, red; nitrogen, blue; phosphorus, orange; sulfur, yellow; water, red spheres; and putative hydrogen bonding interactions, dashed brown lines.

bonding interactions (**Supplementary Fig. 28**). Consistent with a lack of divalent metal influence on PriB catalysis (**Supplementary Fig. 8**), the side chain amines of PriB Arg108 and Lys179 in substrate-bound PriB occupy the divalent-cation-binding site of corresponding metal-dependent PTs (**Fig. 2b**)[20]. PriB substrate orientation in ligand-bound structures is most similar to that of indole C7 PTs (MpnD and TleC; both enzymes display broad donor specificity)[14] and clearly distinct from that of the corresponding C2 (FtmPT1), C4 (FgaPT2) or C3 PTs (CdpNPT) (**Supplementary Fig. 29**) whereas the DMSPP C1 is located within 3.6 Å of the indole C6 or C7 in PriB (**Supplementary Fig. 28**). The unique substrate orientation within PriB and/or the observed PriB-binding-pocket dynamics upon substrate binding are potential contributors to the catalyst's expanded permissiveness. Similar to other indole PTs[22], conserved aromatic residues (Tyr181, Tyr236 and Tyr380) stabilize the prenyl carbocation via π–cation interactions, and a conserved glutamic acid (Glu94) is poised as a general base for indole activation in which the PriB His312 imidazole may further stabilize indole C6 transition-state charge density (**Supplementary Fig. 28**). This histidine is also conserved in some other indole C6-PTs[13] (**Supplementary Fig. 27**).

In summary, genome mining of a microbe associated with an Appalachian underground coal-mine fire enabled the discovery and characterization of the L-Trp C6 C-PT PriB, whose enhanced proficiency and expanded donor–acceptor substrate permissiveness is consistent with similar proficiency and permissiveness among other native or engineered enzymes[23,24]. As a biocatalyst, PriB is robust, and it catalyzes a reaction (indole C6 alkylation) that remains a challenge to conventional synthetic strategies[25]. The permissiveness of PriB (and other PTs) enables complementary synthetic strategies that might be further enhanced via structure-based engineering.

Received 29 June 2016; accepted 1 December 2016;
published online 6 February 2017

Methods

Methods, including statements of data availability and any associated accession codes and references, are available in the online version of the paper.

References

1. Walsh, C.T. *Nat. Chem. Biol.* **11**, 620–624 (2015).
2. Tibrewal, N. & Tang, Y. *Annu. Rev. Chem. Biomol. Eng.* **5**, 347–366 (2014).
3. Gantt, R.W., Peltier-Pain, P. & Thorson, J.S. *Nat. Prod. Rep.* **28**, 1811–1853 (2011).
4. Elshahawi, S.I. *et al. Proc. Natl. Acad. Sci. USA* **110**, E295–E304 (2013).
5. Ling, L.L. *et al. Nature* **517**, 455–459 (2015).
6. Donia, M.S. & Fischbach, M.A. *Science* **349**, 1254766 (2015).
7. Carr, G. *et al. Org. Lett.* **14**, 2822–2825 (2012).
8. Wang, X. *et al. Org. Lett.* **17**, 2796–2799 (2015).
9. Fan, A., Winkelblech, J. & Li, S.-M. *Appl. Microbiol. Biotechnol.* **99**, 7399–7415 (2015).
10. Rudolf, J.D., Wang, H. & Poulter, C.D. *J. Am. Chem. Soc.* **135**, 1895–1902 (2013).
11. Takahashi, S. *et al. J. Bacteriol.* **192**, 2839–2851 (2010).
12. Winkelblech, J. & Li, S.M. *ChemBioChem* **15**, 1030–1039 (2014).
13. Rudolf, J.D. & Poulter, C.D. *ACS Chem. Biol.* **8**, 2707–2714 (2013).
14. Mori, T. *et al. Nat. Commun.* **7**, 10849 (2016).
15. Subramanian, T., Liu, S., Troutman, J.M., Andres, D.A. & Spielmann, H.P. *ChemBioChem* **9**, 2872–2882 (2008).
16. Eisenstein, B.I., Oleson, F.B. Jr. & Baltz, R.H. *Clin. Infect. Dis.* **50** (Suppl. 1): S10–S15 (2010).
17. Unsöld, I.A. & Li, S.-M. *Microbiology* **151**, 1499–1505 (2005).
18. Mahmoodi, N. & Tanner, M.E. *ChemBioChem* **14**, 2029–2037 (2013).
19. Yin, N. *et al. J. Med. Chem.* **58**, 5137–5142 (2015).
20. Kuzuyama, T., Noel, J.P. & Richard, S.B. *Nature* **435**, 983–987 (2005).
21. Bonitz, T., Alva, V., Saleh, O., Lupas, A.N. & Heide, L. *PLoS One* **6**, e27336 (2011).
22. Tanner, M.E. *Nat. Prod. Rep.* **32**, 88–101 (2015).
23. Williams, G.J., Zhang, C. & Thorson, J.S. *Nat. Chem. Biol.* **3**, 657–662 (2007).
24. Nobeli, I., Favia, A.D. & Thornton, J.M. *Nat. Biotechnol.* **27**, 157–167 (2009).
25. Feng, Y. *et al. J. Am. Chem. Soc.* **137**, 10160–10163 (2015).

Acknowledgments

This work was supported by NIH grants R37 AI52188 and R01 CA203257 (J.S.T.), U01 GM098248 (G.N.P.) and NCATS (UL1TR001998). Daptomycin (Cubicin) was generously provided by Merck. We are grateful to J. Rohr, S. Van Lanen and J. Chappell (College of Pharmacy, University of Kentucky) for helpful discussion and facilitating access to shared equipment and/or reagents. We thank the University of Kentucky Mass Spectrometry Facility for the HR–ESI–MS support. This research also used resources of the Advanced Photon Source, a US Department of Energy (DOE) Office of Science user facility operated by Argonne National Laboratory (DE-AC02-06CH11357). Use of the Lilly Research Laboratories Collaborative Access Team (LRL-CAT) beamline at Sector 31 of the Advanced Photon Source was provided by Eli Lilly and Company.

Author contributions

S.I.E. and H.C. contributed to the experimental design and execution and manuscript preparation; K.A.S. and L.V.P. contributed to experimental design and execution; T.S. and H.P.S. contributed experimental reagents and consultation; M.L.F. contributed to experimental design and execution and provided key consultation; G.N.P. and J.S.T. contributed to the experimental design, project oversight and manuscript preparation; S.S. contributed to the experimental design and execution, project oversight and manuscript preparation.

Competing financial interests

The authors declare competing financial interests: details accompany the online version of the paper.

Additional information

Any supplementary information, chemical compound information and source data are available in the online version of the paper. Reprints and permissions information is available online at http://www.nature.com/reprints/index.html. Correspondence and requests for materials should be addressed to S.S., J.S.T. or G.N.P.

ONLINE METHODS

Strains and materials. *Streptomyces* sp. RM-5-8 was isolated from the Ruth Mullins underground coal-mine-fire site and was provided by the University of Kentucky CPRI Natural Products Repository. All primers were purchased from Integrated DNA Technology, *E. coli* 5α and BL21(DE3) competent cells were purchased from New England BioLabs. Dimethylallyl *S*-thiolodiphosphate (DMSPP) was purchased from Echelon Biosciences. Polyethylene glycol 3350 (PEG 3350) and PEG 4000 both in the form of a 50% w/v solution, as well as crystallization screens Index HT, PEGRx HT, Crystal Screen HT and SaltRx HT were obtained from Hampton Research. Crystallization screens JCSG-plus HT-96, Morpheus and MIDAS were from Molecular Dimensions. All other reagents and chemicals were purchased from Sigma-Aldrich or Fisher Scientific and were used without further purification unless otherwise stated. PD-10 columns and Ni-NTA superflow columns were purchased from GE Healthcare. All non-native synthetic prenyl donors were synthesized as previously reported[26,27]. All solvents used were of ACS grade and purchased from Pharmco-Aaper. All DNA sequencing was conducted with the primers T7 promoter (5′-TAATACGACTCACTATAGGG-3′) and T7 terminator (5′-GCTAGTTATTGCTCAGCGG-3′). Daptomycin (DAP, Cubicin) was generously provided by Merck.

General methods. NMR spectra were obtained at ambient temperature on Varian Unity Inova 400, 500 or 600 MHz instruments (University of Kentucky College of Pharmacy NMR facility) using 99.8% d_6-DMSO (Cambridge Isotope Laboratories) as a solvent. Chemical shifts were referenced to internal solvent resonances and are reported in parts per million (p.p.m.) with coupling constants *J* given in Hz. Analytical TLC was performed on silica gel glass TLC plates (EMD Millipore). Visualization was accomplished with UV light (254 nm) followed by staining with vanillin-sulfuric acid reagent and heating. HPLC was accomplished on an Agilent 1260 HPLC system equipped with a DAD detector (HPLC methods A, B and C), a Waters 2695 separation module equipped with a Waters 2996 photodiode array detector and a Waters Micromass ZQ (methods D and E), or a Varian Prostar 210 HPLC system equipped with a photodiode array detector (methods F and G). HPLC peak areas were integrated with Varian Star Chromatography Workstation Software and the percent conversion calculated as a percent of the total peak area. High-resolution electrospray ionization (ESI) mass spectra were recorded on an Exactive Orbitrap mass spectrometer (Thermo Scientific).

HPLC method A: Luna C18 (5 µm, 4.6 mm × 250 mm) column (Phenomenex) [10% B for 5 min, gradient of 10% B to 100% B over 18 min, 100% B for 5 min, 100% B to 10% B over 1 min, 10% B for 4 min (A = double distilled H_2O (ddH_2O) with 0.1% formic acid; B = acetonitrile) flow rate = 1 ml min^{-1}; A_{280}].

HPLC method B: Luna C18 (5 µm, 4.6 mm × 250 mm) column (Phenomenex) [20% B for 5 min, gradient of 20% B to 100% B over 16 min, 100% B for 7 min, 100% B to 20% B over 1 min, 20% B for 4 min (A = ddH_2O with 0.1% formic acid; B = acetonitrile) flow rate = 1 ml min^{-1}; A_{280}].

HPLC method C: Luna C18 (5 µm, 4.6 mm × 250 mm) column (Phenomenex) [10% B for 5 min, gradient of 10% B to 100% B over 10 min, 100% B for 13 min, 100% B to 10% B over 1 min, 10% B for 4 min (A = ddH_2O with 0.1% formic acid; B = acetonitrile) flow rate = 1 ml min^{-1}; A_{280}].

HPLC method D: Kinetex EVO C18 (5µm, 4.6 mm × 250 mm) column (Phenomenex) [10% B for 5 min, gradient of 10% B to 100% B over 21 min, 100% B for 4 min, 100% B to 10% B over 1 min, 10% B for 4 min (A = ddH_2O with 0.1% formic acid; B = acetonitrile with 0.1% formic acid) flow rate = 0.5 ml min^{-1}; A_{280}].

HPLC method E: Kinetex EVO C18 (5 µm, 4.6 mm × 250 mm) column (Phenomenex) [10% B for 5 min, gradient of 10% B to 100% B over 15 min, 100% B for 10 min, 100% B to 10% B over 1 min, 10% B for 4 min (A = ddH_2O with 0.1% formic acid; B = acetonitrile with 0.1% formic acid) flow rate = 0.5 ml min^{-1}; A_{280}].

HPLC method F: Supelco Discovery Bio wide pore C18 (10 µm, 250 × 21.2 mm) column (Sigma-Aldrich) [10% B for 5 min, gradient of 10% B to 100% B over 15 min, 100% B for 10 min, 100% B to 10% B over 1 min, 10% B for 4 min (A = ddH_2O with 0.05% formic acid; B = acetonitrile) flow rate = 8 ml min^{-1}; A_{280}].

HPLC method G: Gemini C18 (5 µm, 10 × 250 mm) column (Phenomenex) [10% B for 2 min, gradient of 10% B to 100% B over 13 min, 100% B for 3 min, 100% B to 10% B for 4 min, 10% B for 4 min (A = ddH_2O with 0.1% trifluoroacetic acid; B = acetonitrile) flow rate: 5.0 ml min^{-1}; A_{280}].

DNA extraction, genome sequencing and analyses. *Streptomyces* sp. RM-5-8 was grown on M2-medium agar (glucose, 4.0 g L^{-1}; Bacto yeast extract, 4.5 g L^{-1}; Bacto malt extract, 10 g L^{-1}; calcium carbonate, 2.0 g L^{-1}; agar, 17.0 g L^{-1}) for four d at 28 °C. Pure colonies were used to inoculate a 250 ml Erlenmeyer flask containing 50 ml of liquid medium A (soluble starch, 20.0 g L^{-1}; glucose, 10.0 g L^{-1}; Bacto peptone, 5.0 g L^{-1}; Bacto yeast extract, 5.0 g L^{-1}; NaCl, 4.0 g L^{-1}; K_2HPO_4, 0.5 g L^{-1}; $MgSO_4$•$7H_2O$, 0.5 g L^{-1}; $CaCO_3$, 2.0 g L^{-1}). After 3 d of incubation at 28 °C with 200 r.p.m. agitation, the cell pellet was collected by centrifugation at 5,000 × *g* for 15 min. Genomic DNA was extracted using an UltraClean Microbial DNA Isolation Kit (MoBio laboratories, Inc) following the manufacturer's protocol. DNA quality and concentration were assessed using gel electrophoresis and Nanodrop 2000c spectrophotometer (Thermo Scientific), and purity was confirmed using 16S rRNA analysis. The resultant DNA solution was subjected to massively parallel sequencing using MiSeq sequencer (Illumina) at the University of Kentucky Advanced Genetic Technologies Center (UK-AGTC). The genome (10.5 Mb, 28× coverage) was assembled using Newbler v.2.9 (Roche Diagnostics). Low-quality regions were sequence verified by polymerase chain reaction and Sanger sequencing. Putative prenyltransferase (PT) genes were identified via Basic Local Alignment Search Tool (BLAST) comparison of the final assembly to a group of 52 fungal and bacterial PT genes (**Supplementary Fig. 3**). Homology searches of the generated contigs were carried out using the BLASTX and position-specific iterated BLAST (PSI–BLAST). Gene alignments and analyses were performed using Geneious Pro 5.0.3 (ref. 28) (**Supplementary Table 1** and **Supplementary Fig. 1**). The sequence of the putative *pri* biosynthetic gene cluster of **2** has been deposited under GenBank accession number KT895008.

Gene cloning and protein production and purification. The *priB* gene was amplified from *Streptomyces sp.* RM-5-8 genomic DNA using the primers PriB-NdeI-F AGGCCATATGGGAGGTCCGATGAGCGGTTTCCA and PriB–HindIII-R TATTAAGCTTTCACAGCCGTGCCCGCGCCCGGTC (engineered restriction sites underlined). The corresponding fragment was cloned into the *E. coli* expression vector pET28a (Novagen) and confirmed via sequencing. The validated expression plasmid (pSEPriB) was subsequently transformed into *E. coli* BL21 (DE3) competent cells (New England BioLabs). Production strains for the group of previously reported fungal and bacterial PTs were constructed in a similar fashion from synthetic genes (GenScript); **Supplementary Table 8**). All studies employed the corresponding N-terminal-His_6 fusion proteins.

For protein production, 1 L of LB medium (Becton, Dickinson and Company) supplemented with kanamycin (50 µg ml^{-1}) was inoculated with 0.1% (v/v) of an overnight pSEPriB-*E. coli* BL21 (DE3) seed culture and grown at 37 °C with shaking (225 r.p.m.). Cultures were induced at an optical density at 600 nm (OD_{600}) of ~0.6–0.8 with isopropyl-β-D-thiogalactopyranoside (IPTG, 0.5 mM final concentration) and allowed to grow for an additional 16 h at 22 °C. Cells were harvested by centrifugation and stored in lysis buffer (10 mM imidazole, 50 mM sodium monobasic phosphate, 300 mM NaCl, pH 8.0) at −80 °C until used. All subsequent steps were carried out on ice. Cells were allowed to thaw and were subsequently lysed by sonication (Virtis VirSonic 475 with a microtip, 100 W, 10 × 10 s pulses, 20 s between pulses). Insoluble debris was removed by centrifugation at 15,000 × *g* for 1 h. The supernatant was collected and filtered using 0.22 µm filters and the desired *N*-His_6–PriB fusion protein was purified via HiTrap nickel–nitrilotriacetic acid (Ni–NTA) affinity chromatography using standard protocols with AKTA Purifier 10 (GE Healthcare). Buffer exchange of each sample was performed using a PD-10 column (GE Healthcare) eluted with 50 mM Tris, 100 mM NaCl, pH 8.0 to yield 5 mg L^{-1} PriB. Fractions were collected and concentrated using Amicon Ultra Centrifuge columns 30,000 MWCO (EMD Millipore) and stored in 50 mM Tris, 100 mM NaCl, pH 8.0 at −80 °C. Protein concentrations were determined by Bradford assay (Bio-Rad) using bovine serum albumin as a standard. Purity and presence of proteins were confirmed by SDS–PAGE gel

doi:10.1038/nchembio.2285

electrophoresis. The *N*-His_6-PriB fusion protein (referred to as PriB) was used for all studies. Production of other PTs for the overall study (**Supplementary Table 8**) followed the same protocol.

Analytical assays and enzyme kinetics. Standard PriB *in vitro* assays were conducted in 1.5 ml tubes in a volume of 100 µl Tris 50 mM (pH 8.0) containing a final concentration of 0.5 mM L-Trp, 1 mM DMAPP, and 250 nM PriB. After pre-incubation of the reaction mixture at 37 °C for 10 min, the reactions were initiated by the addition of enzyme and allowed to proceed for 60 min (unless otherwise noted) at 37 °C. The reactions were quenched by the addition of 100 µl MeOH and mixing followed by centrifugation (22,000 × *g*, 15 min, 4 °C) to remove precipitated protein. The supernatants were analyzed by HPLC using method A (see "General methods") to calculate conversion rate based on the area of substrate and the prenylated product peaks. When applicable, subsequent product mass analyses (**Supplementary Tables 5** and **6**; **Supplementary Note**) were typically accomplished via direct LC–MS (LC–ESI–MS, method D or E, see "General methods") and/or HR–ESI–MS of HPLC-purified products (method A).

Temperature optimization. Replicates of the standard assay were conducted at 4, 10, 20, 30, 37, 45, 55, 65 °C.

pH optimization. Replicates of the standard assay were modified via substitution of Tris 50 mM (pH 8.0) with 50 mM citric acid–sodium dihydrogen phosphate (pH 3.5–8.0) or 50 mM glycine–sodium hydroxide (pH 8.5–11.0).

Various cation assessment. Replicates of the standard assay were conducted in the presence of 5 or 10 mM of each of the following: EDTA, $MgCl_2$, $CuCl_2$, $MnCl_2$, LiCl, $BaCl_2$, $CoCl_2$, $CaCl_2$, $ZnCl_2$, and $SrCl_2$.

Determination of kinetic parameters. Replicates of the standard assay were used with variable acceptor ([L-Trp] = 1 × 10^{-3}–5 mM) and fixed donor ([DMAPP] = 1 mM) or variable donor ([DMAPP] = 0.5–4 mM) and fixed acceptor ([L-Trp] = 0.5 mM) in triplicate. The kinetic constants were calculated by nonlinear regression fit to the Michaelis–Menten equation using GraphPad Prism 7 software.

PriB substrate specificity. Replicate assays were performed with 0.5 mM acceptor and 0.3–2 mM donor in the presence of 2 µM purified PriB in 50 mM Tris pH 8.0 for 16 h.

Daptomycin catalyst survey. Replicates assays contained 1 µM enzyme, 1 mM DAP, and 1 mM DMAPP in the presence of 50 mM Tris (pH 8.0). Assays containing FgaPT2 or CdpNPT were supplemented with 10 mM $CaCl_2$.

Prenylated L-Trp product isolation/characterization. For isolation and full characterization of prenylated Trp analogs, 0.5 ml reactions (×20) in 1.5 ml Eppendorf tubes containing 2.5 mM acceptor (L-Trp or 6-methyl-DL-Trp), 2.5 mM DMAPP, 5 µM enzyme (PriB or FgaPT2) in 50 mM Tris (pH 8.0) were incubated for 16 h at 37 °C. Divalent cation (10 mM $CaCl_2$) was also included in all FgaPT2-catalyzed reactions. Reactions were combined, terminated by mixing with equal volume of MeOH, centrifuged to remove precipitated protein and dried under reduced pressure. The crude reaction mixture was redissolved in MeOH and purified via preparative HPLC (Method F).

4-dimethylallyl-L-Trp (*70*). White solid (5.6 mg, 56% isolation yield); (+)-ESI–MS: *m/z* 273 $[M + H]^+$; (+)-HR–ESI–MS: *m/z* 273.1596 $[M + H]^+$ (calculated for $C_{16}H_{20}N_2O_2$, 273.1598). ^1H NMR (d_6-DMSO, 400 MHz) and ^{13}C NMR (d_6-DMSO, 100 MHz); see **Supplementary Figure 26**; **Supplementary Table 9**; **Supplementary Note**.

6-dimethylallyl-L-Trp (*1*). White solid (8 mg, 80% isolation yield); (+)-ESI–MS: *m/z* 273 $[M + H]^+$; (+)-HR–ESI–MS: *m/z* 273.1598 $[M + H]^+$ (calculated for $C_{16}H_{20}N_2O_2$, 273.1598). ^1H NMR (d_6-DMSO, 400 MHz) and ^{13}C NMR (d_6-DMSO, 100 MHz); see **Supplementary Figure 9**; **Supplementary Table 2**; **Supplementary Note**.

6-methyl-7-dimethylallyl-L-Trp (*69*). White solid (6 mg, 15% isolation yield); (+)-ESI–MS: *m/z* 287 $[M + H]^+$; (+)-HR–ESI–MS: *m/z* 287.1753 $[M + H]^+$ (calculated for $C_{17}H_{23}N_2O_2$, 287.1754). ^1H NMR (d_6-DMSO, 400 MHz) and ^{13}C NMR (d_6-DMSO, 100 MHz); see **Supplementary Figure 9**; **Supplementary Table 3**; **Supplementary Note**.

Prenylated DAP product isolation and characterization. For isolation and full characterization of prenylated DAP analogs, reactions containing 1 mM DAP, 1 mM DMAPP and 1 µM enzyme (PriB, FgaPT2 or CdpNPT) in 50 µl Tris (pH 8.0) were incubated for 12 h at 37 °C. FgaPT2- and CdpNPT-catalyzed reactions also contained divalent cation (10 mM $CaCl_2$). Reactions were terminated by mixing with equal volume of MeOH, centrifuged to remove precipitated protein and dried under reduced pressure. Crude reaction mixtures were subsequently redissolved in MeOH and purified via preparative HPLC (method G).

6-C-prenyl-Trp$_1$ DAP (*66*). White solid (0.6 mg, 6% isolation yield); (−)-ESI–MS: *m/z* 1687 $[M - H]^-$; (−)-HR–ESI–MS: *m/z* 1686.7635 $[M - H]^-$ (calculated for $C_{77}H_{108}N_{17}O_{26}$, 1686.7657). ^1H NMR (d_6-DMSO, 600 MHz) and ^{13}C NMR (d_6-DMSO, 150 MHz); see **Supplementary Figures 22–24**, **Supplementary Table 8**; **Supplementary Note**.

N-prenyl-Trp$_1$ DAP (*67*). White solid (6 mg, 60% isolation yield); (−)-ESI-MS: *m/z* 1687 $[M - H]^-$; (−)-HR-ESI-MS: *m/z* 1686.7603 $[M - H]^-$ (calculated for $C_{77}H_{108}N_{17}O_{26}$, 1686.7657); (+)-HR–ESI–MS: *m/z* 1688.7870 $[M + H]^+$ (calculated for $C_{77}H_{110}N_{17}O_{26}$, 1688.7802); ^1H NMR (d_6-DMSO, 400 MHz) and ^{13}C NMR (d_6-DMSO, 100 MHz); see **Supplementary Figures 22–24**, **Supplementary Table 8**; **Supplementary Note**.

CdpNPT prenylated daptomycin mixture (*67*/*68*). White solid (53 mg, 70% isolation yield, mixture 1:1); (−)-ESI–MS: *m/z* 1687 $[M - H]^-$; (−)-HR–ESI–MS: *m/z* 1686.7655 $[M - H]^-$ and $[(M - H_2O) - H]^-$ (calculated for $C_{77}H_{108}N_{17}O_{26}$, 1686.7657); ^1H NMR (d_6-DMSO, 400 MHz) and ^{13}C NMR (d_6-DMSO, 100 MHz); see **Supplementary Figures 22–24**; **Supplementary Table 8**; **Supplementary Note**.

Bioactivity assays. All DAP and DAP analog stocks were calibrated by absorbance (ε_{366} = 4,000 L mol^{-1} cm^{-1}) (ref. 29) and all bioactivity assays were conducted in triplicate. Antimicrobial activities were determined by following a previously reported protocol[30]. Strain growth also followed our prior protocol[30] in which LB medium (BD244620) was used for *Bacillus subtilis* and Middlebrook 7H9 with OADC enrichment (Sigma-Aldrich) for *Mycobacterium aurum*. Cancer cell line cytotoxicity assays as a measure of general eukaryotic cell toxicity employed the human lung nonsmall-cell carcinoma cell line A549 as previously reported[30].

Crystallization, diffraction data collection, and structure determination of PriB. PriB from Ni-affinity chromatography was further purified via gel filtration (Superdex 200; 50 mM Tris pH 7.5 buffer, 100 mM NaCl) via an AKTAprime Plus FPLC system (GE Healthcare), concentrated with Amicon Ultra-4 Centrifugal Filter Units (EMD Millipore) to a final concentration of 34 mg ml^{-1}, drop flash-frozen and stored at −80 °C before use. Initial crystallization trials were set up by mosquito Crystal nanoliter dispenser robot (TTP Labtech) on MRC 2 Well crystallization plates (Hampton Research) using sitting drop vapor-diffusion method testing against all seven commercial high-throughput screens each with 96 conditions. PriB was crystallized by sitting drop vapor diffusion using a 1:1 v/v mixing of 10 mg ml^{-1} PriB solution in the presence of 1 mM L-Trp with reservoir solution containing 0.1 M Tris, pH 8.5, 20% w/v PEG 3350, 0.1 M $MgCl_2$. The mixed drops of 0.4–1 µl were equilibrated over a reservoir solution of 50 µl and incubated at 20 °C in the dark. Monoclinic shaped crystals grew after 6–10 d with the longest dimension typically reaching 100–600 µm. The iodine derivative was prepared by soaking a solution of 0.5 M sodium iodide, 50 mM Tris pH 8.5, 10% w/v PEG 3350, 0.05 M $MgCl_2$ into a drop of PriB crystals (grown under the same condition as the apo form) at a 1:3 v/v mixing ratio. The ternary complex was obtained by soaking a solution of 25 mM substrate mimic dimethylallyl *S*-thiolodiphosphate (DMSPP), 50 mM Tris, pH 8.5, 10% w/v PEG 3350, 0.05 M $MgCl_2$ into PriB crystals (grown under conditions similar to the native form in the presence of substrate 1 mM L-Trp at pH 8.0) at a 1:1.5 v/v mixing ratio. The product diphosphate-bound form was obtained by growing PriB crystals using the same sitting drop procedure but under different conditions by 1:1 v/v mixing of 10 mg ml^{-1} PriB solution in the presence of 1 mM of each of dimethylallyl diphosphate and daptomycin with reservoir conditions containing 100 mM Tris, pH 8.0, 28% w/v PEG 4000. Crystals of the native form and ternary complex were cryoprotected by transferring into MiTeGen's LV CryoOil (MiTeGen) and flash-frozen in liquid nitrogen. The crystal of the diphosphate complex was directly flash frozen in liquid nitrogen without additional cryoprotectant.

Diffraction data were collected at the Advanced Photon Source at Argonne National Laboratory on the LRL-CAT (31-ID-D) beamline. The detector used was a Rayonix 225 HE CCD (Rayonix) using a single wavelength of 1.3776 Å for the iodine derivative and 0.97931 Å for all other data sets. The anomalous data set was collected and processed to a resolution of 1.54 Å, the apo form to 1.15 Å, the ternary complex to 1.4 Å, and the diphosphate complex to 1.5 Å (**Supplementary Table 11**). The anomalous and apo data sets were indexed, integrated, and scaled using XDS[31]. The substrate/product complexes data sets were indexed and integrated by MOSFLM, scaled and merged by SCALA from the CCP4 program suites[32]. The structure of PriB was determined by single-wavelength anomalous diffraction (SAD) phasing on the iodine derivative data set using AutoSol from the PHENIX software suite[33]. One copy of the polypeptide was found and built in the asymmetric unit with 26 iodine atoms of various occupancy. The sparsity of intermolecular contacts (largest interface area <530 Å^2) in the crystal packing suggest the protein is a monomer. Analysis of crystal contact suggests the protein to be a monomer. The protein model as traced from the iodide containing data set was then used as the search model for solving the apo and ligand complexes by molecular replacement with Phaser_MR and Autobuild of the PHENIX suite[33]. Most of the amino acid residues were successfully built with traceable electron density except for short stretches at the N and C termini, as well as one short flexible loop away from the active site. Ligands and alternative conformations of residues were built into the model based on difference electron density maps. The structures were completed with alternating rounds of manual model building with COOT[34] and refinement with PHENIX. Water was added and updated during refinement. The final structures were refined to the same resolution limits as in data collection with favorable R_{cryst} and R_{free} values (**Supplementary Table 11**). Model quality was assessed using MolProbity[35]. Ramachandran statistics determined as the percentage of residues were 98.9, 1.1, 0.0 in the most favored, additionally allowed and outlier regions of the Ramachandran diagram, respectively. All structures were rendered using PyMOL[35].

Data availability. Nucleotide sequence data for the *pri* cluster is available under GenBank accession code KT895008. The PriB X-ray crystal structures were deposited at the Protein Data Bank: the PriB–L-Trp–dimethylallyl *S*-thiolodiphosphate ternary complex (5INJ), the apo structure (5JXM), and the PriB–pyrophosphate binary complex (5K9M). All other data generated or analyzed during this study are included in this published article (and its supplementary information files) or are available from the corresponding author on reasonable request.

26. Chehade, K.A.H. *et al. J. Am. Chem. Soc.* **124**, 8206–8219 (2002).
27. Subramanian, T., Wang, Z., Troutman, J.M., Andres, D.A. & Spielmann, H.P. *Org. Lett.* **7**, 2109–2112 (2005).
28. Kearse, M. *et al. Bioinformatics* **28**, 1647–1649 (2012).
29. Debono, M. *et al. J. Antibiot. (Tokyo)* **41**, 1093–1105 (1988).
30. Shaaban, K.A. *et al. J. Nat. Prod.* **78**, 1723–1729 (2015).
31. Kabsch, W. *Acta Crystallogr. D Biol. Crystallogr.* **66**, 125–132 (2010).
32. Collaborative Computational Project, Number 4. *Acta Crystallogr. D Biol. Crystallogr.* **50**, 760–763 (1994).
33. Adams, P.D. *et al. Acta Crystallogr. D Biol. Crystallogr.* **66**, 213–221 (2010).
34. Emsley, P., Lohkamp, B., Scott, W.G. & Cowtan, K. *Acta Crystallogr. D Biol. Crystallogr.* **66**, 486–501 (2010).
35. Chen, V.B. *et al. Acta Crystallogr. D Biol. Crystallogr.* **66**, 12–21 (2010).

doi:10.1038/nchembio.2285